Ln$_{1-x}$A$_x$CoO$_3$ (Ln = Er, La; A = Ca, Sr)/Carbon Nanotube Composite Materials Applied for Rechargeable Zn/Air Batteries

Anke Weidenkaff,*,[†] Stefan G. Ebbinghaus,[†] and Thomas Lippert[‡]

Solid State Chemistry, University of Augsburg, D-86159 Augsburg, Germany, and Department General Energy Research, Paul Scherrer Institute, CH-5232 Villigen, Switzerland

Received December 13, 2001. Revised Manuscript Received January 25, 2002

Calcium- and strontium-substituted rare earth cobaltate powders with the perovskite structure (ABO$_3$) are synthesized by coprecipitation, ceramic, complexation, and microemulsion processes. On these metal oxide particles, a carbon nanotube composite material was prepared by a catalytic hydrocarbon dissociation reaction. The material was tested for a possible application as an oxygen electrode in zinc/air batteries. Through a systematic characterization of the produced materials, the common strategy of screening processes for new materials can be replaced by the tailoring of an optimized functional material. To study the influence of the synthesis route and substitution at the A site on the crystallographic structure, the materials were characterized by X-ray diffraction (XRD) and electron microscopy (EM). Phase formation, reactivity, and stability were monitored by high-temperature X-ray diffraction and thermoanalytical (TA) experiments. The electrochemical activities of the samples for oxygen evolution was measured in a three-electrode arrangement.

Introduction

Perovskite-type metal oxides (with the ABO$_3$ structure) are known to be low-cost and active electrocatalysts for practical applications in fuel cells and metal/air batteries.[1] Among these Zn/air batteries are high-specific-energy and environmentally friendly batteries. After discharge, however, the oxidized ZnO electrode has to be exchanged, which is a disadvantage of the system. This is the motivation for the development of an electrode that allows the electrical recharging of Zn/air batteries.

During the charging of the battery, ZnO is reduced to Zn, while oxygen is released at the air electrode. During discharge, oxygen from the air has to be reduced to OH$^-$ on the air electrode to react with Zn to form ZnO and water in the alkaline solution. The development of oxygen-electrode materials that operate well in both modes will play a key role in the technical realization of electrically rechargeable air-based batteries and in solid oxide fuel cell technologies. Efforts to develop oxygen-electrode catalysts that will operate in both anodic and cathodic modea are confronted with one major problem: The oxygen reduction and generation reactions in aqueous media are irreversible [E(O$_2$ generation) > E(O$_2$ reduction)], even at moderate temperatures. This irreversibility causes efficiency losses and lifetime problems for the catalyst and its support material. Suitable electrocatalyst candidates have been studied and identified among the perovskites, and it was found that Ca- or Sr-substituted lanthanum cobaltates show the best performance.[2,3]

The structure of LaCoO$_3$ is described as a slightly distorted rhomboedral perovskite structure. Substitution in the La position is possible up to a certain extent without destruction of the perovskite structure.[4]

In refs 3 and 4, it was shown that the conductivity increases with increasing Ca content. This was related to the higher density of charge carriers and the reduced Co−Co distance. An important parameter for the electronic properties of perovskite-based electrocatalyst materials is probably also the valance of the B cation, which is determined by the ratio between the contents of La and Ca cations and oxygen. According to simple ionic considerations, upon substitution of three-valenced La by two-valenced Ca or Sr, the Co cations should be partly oxidized to the unusual oxidation state of +4. Co^{4+}, however, is not stable and can be reduced by lattice oxygen.[5] This would result in oxygen vacancies maintaining the electrical neutrality.

To increase the catalytic activity, various synthesis methods such as sol−gel processes, spray pyrolysis, microemulsion, and complexing techniques have been developed to enhance the surface area of the metal oxides.

The bifunctional air electrode consists of perovskite powder mixed with carbon black. Small carbon particles are used as the support material because of their electrical properties and high surface area. The two

---

* To whom correspondence should be addressed.
† University of Augsburg.
‡ Paul Scherrer Institute.

(1) McEvoy, A. J. *J. Mater. Sci.* **2001,** *36,* 1087−1091.

(2) Müller, S.; Striebel, K.; Haas, O. *Electrochim. Acta* **1994,** *39,* 1661−1668.

(3) Kahoul, A.; Hammouche, A.; Naamoune, F.; Chartier, P.; Poilerat, G.; Koenig, J. F. *Mater. Res. Bul.* **2000,** *35,* 1955−1966.

(4) Ohno, Y.; Nagata, S.; Sato, H. *Solid State Ionics* **1983,** *9−10,* 1001−1008.

(5) Tanaka, H.; Misono, M. *Curr. Opin. Solid State Chem. Mater. Sci.* **2001,** *5,* 381−387.

components are pressed onto a Teflon-bonded electrode. State-of-the-art bifunctional oxygen/air electrodes show a difference of approximately 800 mV between oxygen reduction and evolution.[2] The composite material is used in a highly alkaline solution, which leads to corrosion problems mainly with the carbon support. The motivation for the work described in this paper is to enhance the efficiency of the battery, which means lowering the overvoltage at the air electrode and increasing the stability of the electrode. Consequently, it is necessary to investigate stable new catalytically active materials, as well as synthesis routes, systematically to create nanometer-sized catalyst particles that are homogeneously dispersed in a conductive and stable support material.

To optimize both the interface between the carbon and the perovskite electrocatalyst and the stability of the electrode, a new composite material was developed. Through the combination of the properties of perovskite and carbon nanotubes in a carbon nanotube/metal oxide composite and the development of a joint production process, the time-consuming purification process for carbon nanotubes is rendered obsolete. Additional experiments were performed to tailor the nano- (nanometer-scale) as well as the macro- (centimeter-scale) structure of the electrodes. As macrostructured templates, cotton fibers were used, but this approach can be extended to the utilization of cotton fiber webs (textiles). The new nanocomposite material can be composed of carbon nanotubes embedded in a matrix of perovskite particles or perovskite particles covered with carbon nanotubes. In this study, we tested the latter case.

Experimental Section

Synthesis of Perovskite Powders. For the electrode material, perovskite powders were produced by using different preparation methods.

Ceramic Methods. With conventional solid-state reactions, coarse materials of the compositions $LaCoO_3$, $La_{0.8}Ca_{0.2}CoO_3$, $La_{0.6}Ca_{0.4}CoO_3$, $La_{0.8}Sr_{0.2}CoO_3$, and $La_{0.6}Sr_{0.4}CoO_3$ were formed. The compounds were prepared by grinding preheated powders of the metal oxides or carbonates (La_2O_3, $CaCO_3$ or $SrCO_3$, and Co_3O_4). The mixtures were then heated at 1300 °C for 48 h with two intermediate grinding procedures. Slow (50 °C/h) or fast (400 °C/h) cooling to room temperature led to different crystallographic structures.

By mixing the components on a molecular level, the formation of the perovskite proceeds at lower temperatures. This can be achieved by dissolving appropriate amounts of metal nitrates; evaporating the solutions to dryness; calcinating the residues in air at 500 °C; and finally, sintering at 1000 °C for 48 h.

Coprecipitation. The metal ions can also be mixed by coprecipitation. Lanthanum, calcium, strontium, and cobalt nitrates with the desired stoichiometry were mixed with a precipitation agent (oxalic acid, ammonia, or tetramethylammonia). The precipitate was minced in an ultrasonic bath, removed by centrifugation, washed several times with acetone, dried, and calcinated at 700 °C for 15 h.

The size of the agglomerated precipitate can be tailored by using inverse micelles as reactors for the precipitation. Stable dispersions of aqueous droplets were produced by stirring a mixture of an oil phase, surfactant, and an aqueous phase. The system is stabilized by the surfactant molecules at the water−oil interface. Two such emulsions, one containing the metal nitrates and the other containing the precipitation agent, were prepared. Upon mixing of the two emulsions, a homogeneous precipitate formed inside the micelles.

For the microemulsions, 0.5 M aqueous solutions of the metal nitrates in stoichiometric ratios were premixed. The single-phase region of the microemulsions was determined visually by titrating a specific amount of, for example, nonylphenyl polyethylene glycol and *n*-octane with the solution of metal nitrates. After the formation of a transparent solution, the microemulsion with the precipitation agent (either ammonia, tetramethylammonia, or oxalic acid) was added. The mixture was stirred for 12 h. The precipitated fine powder was separated by centrifugation, washed several times with acetone, dried, and calcinated at 700 °C for 15 h.

Pechini Method. Metal complexes with organic ligands were prepared as precursors for the metal oxides. In the hydroxy carbon acid-aided synthesis often referred to in the literature as the Pechini method,[6,7] citric acid or tartaric acid is used as the complexing agent.

A stoichiometric amount of hydroxy acid was added to the solution of the Lanthanum, calcium, strontium, and cobalt nitrates with the desired stoichiometry. Water was rotoevaporated at 50 °C until a sol was formed. The product was further dehydrated either by freeze-drying or in a vacuum at 50 °C. The obtained solid amorphous precursor was decomposed and calcinated at various temperatures between 600 and 800 °C. The decomposition and oxidation were monitored by thermogravimetry and mass spectroscopy.

Cotton fibers were treated with 100% nitric acid to give a highly explosive nitrocellulose in a procedure similar to that described in ref 8. In distinction from the published process, however, the prepared cotton fiber in our experiments was soaked with the tartrate precursor solution before the combustion process so that a nanostructured material of ternary metal oxides could be obtained.

Synthesis of Composite Materials. For the production of the carbon nanotube/metal oxide composite material, perovskite powders or macrostructured agglomerates (textile templates) were coated with a citrate precursor containing the perovskite mixture with a slight excess of cobalt oxide (<1%). The particles were inserted into the isothermic zone of a fixed-bed continuous-flow reactor (described in ref 9). At the reaction temperature (700 °C), acetylene (100 mL/min) decomposed to form carbon nanotubes. The reaction time was 3 min.

Sample Characterizations. The quality of the polycrystalline products was studied by various methods, as described below.

The structural analysis of the perovskites powders and composite materials was performed with X-ray diffraction (XRD) data collected on a Seifert XRD 3003-TT diffractometer using Cu K_α radiation. High-temperature X-ray diffraction (HT-XRD) studies were performed on an Enraf Nonius XRD diffractometer with Co K_α radiation and a 120° PSD detector. For the temperature calibration, a silicon standard was used.

The morphology of the samples was examined using a LEO Gemini 982 scanning electron microscope (SEM) equipped with a Röntec energy-dispersive X-ray analysis (EDX) detector system. Transmission electron microscopic (TEM) studies and electron diffraction were done on a Phillips CM 30 instrument.

Thermogravimetric/mass spectrometric (TGA/MS) studies were performed with a Netzsch TA 409 system monitoring a thermogravimetric (TG) and differential thermal analysis (DTA) or differential scanning calorimetric (DSC) signal. The thermobalance was connected by skimmer to a mass spectrometer (MS).

(6) Baythoun, M. S. G.; Sale, F. R. *J. Mater. Sci.* **1982**, *17*, 2757−2769.

(7) Teraoka, Y.; Kakebayashi, H.; Moriguchi, I.; Kagawa, S. *Chem. Lett.* **1991**, 673−676.

(8) Kharton, V. V.; Figueiredo, F. M.; Kovalevsky, A. V.; Viskup, A. P.; Naumovich, E. N.; Yaremchenko, A. A.; Bashmakov, I. A.; Marques, F. M. B. *J. Eur. Ceram. Soc.* **2001**, *21*, 2301−2309.

(9) Weidenkaff, A.; Ebbinghaus, S.; Mauron, P.; Reller, A.; Zhang, Y.; Züttel, A. *Mater. Sci. Eng. C* **2001**, *19*, 119−123.
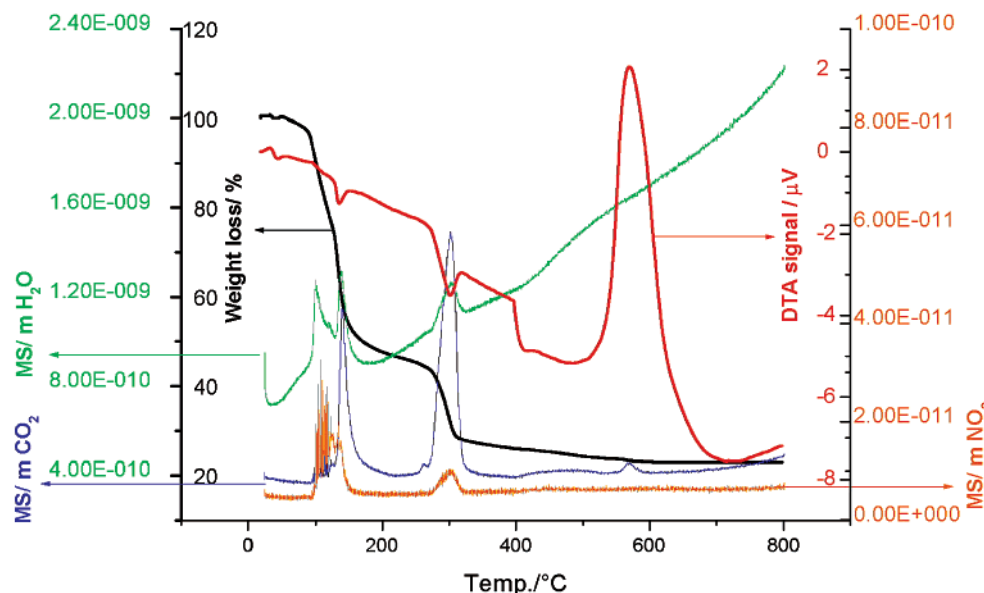
Figure 1. TG-MS plot for the decomposition of the amorphous citrate precursor of $La_{0.6}Ca_{0.4}CoO_3$.

The surface area measurements were done by the BET method (Micrometrics ASAP 2000).

After preparation and characterization of the perovskites, electrodes were produced and tested for catalytic activity in an electrochemical treatment. The tests of the electrodes were performed during several charge and discharge processes[2] in a three-electrode arrangement.

Results and Discussion

Phase Formation and Phase Analysis. To study the influence of A-site cation substitution on the structure and the properties of the perovskites Ca-, Ba-, Sr-, and Er-substituted lanthanum cobaltate particles were formed by ceramic methods, decomposition of metal organic complexes (amorphous citrate/tartrate complexes), and precipitation of hydroxides and oxalates. The phase formation process was monitored with the described methods for the different precursors.

Ceramic Method. The minimum temperature for phase formation of the lanthanum cobaltates from the oxides was 1300 °C for at least 48 h. It was not possible to produce lanthanum cobaltates with a Ca substitution of more than 40%. The evaporation of the mixed metal nitrate led to crystals of red-orange color (see Figure 3a), which decomposed to black metal oxides.

Coprecipitation. The coprecipitation and calcination of water-insoluble hydroxides and oxalates in aqueous solution led to coarse particles. Because of the different solubilities of the precipitates and the intermediate formation of soluble metal complexes, it was difficult to achieve the complete and homogeneous precipitation of the metal ions. Most of these experiments led to multiphase products that were not used further. By using reverse emulsions as microreactors, single-phase products with the compositions $La_{0.6}Ca_{0.4}CoO_3$ and $La_{0.6}Sr_{0.4}CoO_3$ were produced. The calcination of the precursors to form the perovskite particles was monitored by TGA, and it was found that the calcination temperatures of the hydroxides from the microemulsion process were 100−200 °C lower than the hydroxide decomposition temperatures of a similar macroemulsion process.

Pechini Method. The formation of metal oxide phases from amorphous citrate and tartrate complex precursors was monitored by HT-XRD, TA, and SEM for the perovskite-type compounds $(La, Er)_{1−x}(Ca, Sr)_xCoO_3$ ($x = 0, 0.2, 0.4,$ and 0.5) and Co_3O_4. Thermogravimetric studies with on-line gas analysis of the decomposition of the citrate complexes showed that the measured weight loss for the $La_{0.6}Ca_{0.4}CoO_3$ precursor was 76.2% of the original weight. Because the exact chemical structure of the citrate precursor (polymeric structure) is not known, the theoretical weight loss for the pure metal citrate can only be estimated to be in the range of 71 mass %. Gas analysis during decomposition showed signals for $m/e = 18$ (H_2O^+), 30 (NO^+), 44 (CO_2+, N_2O^+), and 46 (NO_2+) (see Figure 1), thus confirming that the precursor contains nitrate in addition to citrate ions. The detected evolution of water can result from the citrate molecule or from crystal water in the compound.

Exothermic two-step decomposition of the nitrate/citrate complexes takes place in the temperature range 100 °C $< T <$ 300 °C. The initial weight loss is due to the dehydration process [see $m/e = 18$ (H_2O^+)]. At $T >$ 100 °C, the precursor decomposes with an enormous volume expansion (>900%). For the removal of nitrate and citrate, a decomposition temperature of 300 °C is necessary. The crystallization and formation of the perovskite phase can be monitored by DTA and occurs between 400 and 600 °C (no mass change detected), which was also confirmed by high-temperature XRD and TEM.

The tartrate and citrate amorphous precursors differ in color: The tartrate complex is pink, whereas the citrate complex is violet. The two-step decomposition of the tartrate complex monitored by TA showed a decomposition temperature of 300 °C and an overall weight loss of 64.4%. The crystallized products exhibited no differences in their XRD patterns. The surface area measured by BET was 15 m²/g, on average, for all products.

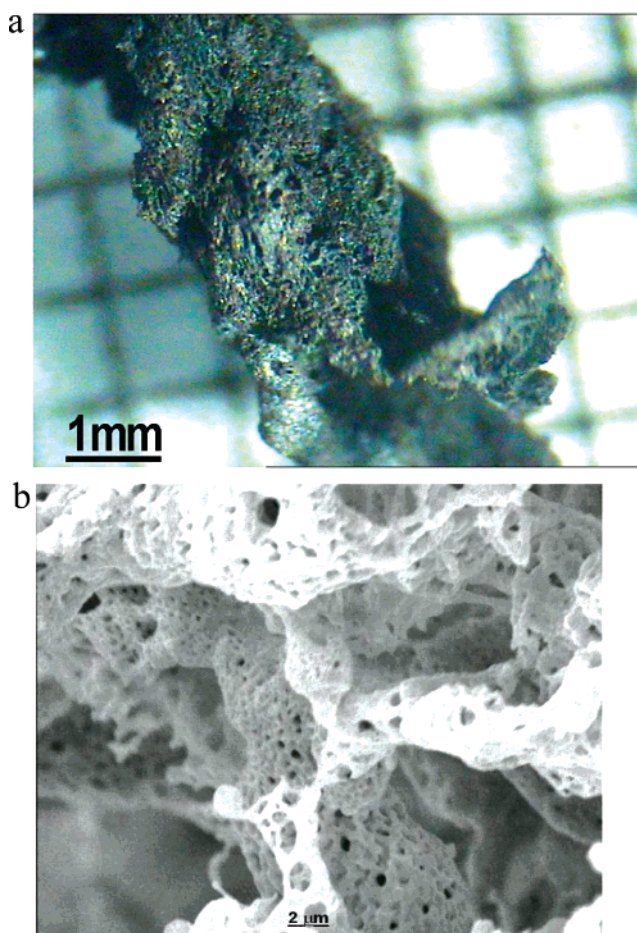The effects of variations in the synthesis parameters, such as the pH of the precursor solution, the addition

Figure 2. (a) Light microscopic picture and (b) scanning electron micrograph of a part from a $La_{0.6}Ca_{0.4}CoO_3$ cord.

Figure 3. Light and scanning electron micrograph of $La_{0.6}$-$Ca_{0.4}CoO_3$ prepared by decomposition of mixed nitrate crystals.

of polymers, the form and amount of complexation agent, the dissociation time, and the temperature, as well as in the cooling procedures were studied in several experiments. In summary, it can be concluded that the pH had to be adjusted carefully to a value of 2 for a monophase product to be obtained. The addition of polymers such as polyethylene glycol exhibited no influence on the structure and morphology of the products in our experiments.

The macrostructure can be defined, for example, by soaking a structure-modified cotton filament (nitrocellulose) with the precursor before the combustion process. The macroscopic form of the fiber remains (see Figure 2a) after decomposition of the precursor. The microstructure of the product shows pores of different sizes (shown in Figure 2b).

All samples studied were monophasic according to their X-ray powder patterns. High-resolution transmission electron micrographs showed the well-crystallized structure of the perovskite and the homogeneity of the structure.

The EDX studies revealed (semiquantitatively) that the individual particles had the compositions given by their chemical formulas.

The morphology of the perovskite particles depended strongly on the synthesis procedure. The products from the ceramic synthesis route were powders with particle diameters of >5 μm. Because of the high synthesis temperatures ($T > 1200$ °C), the powders were sintered to form coarse round-shaped particles with low surface

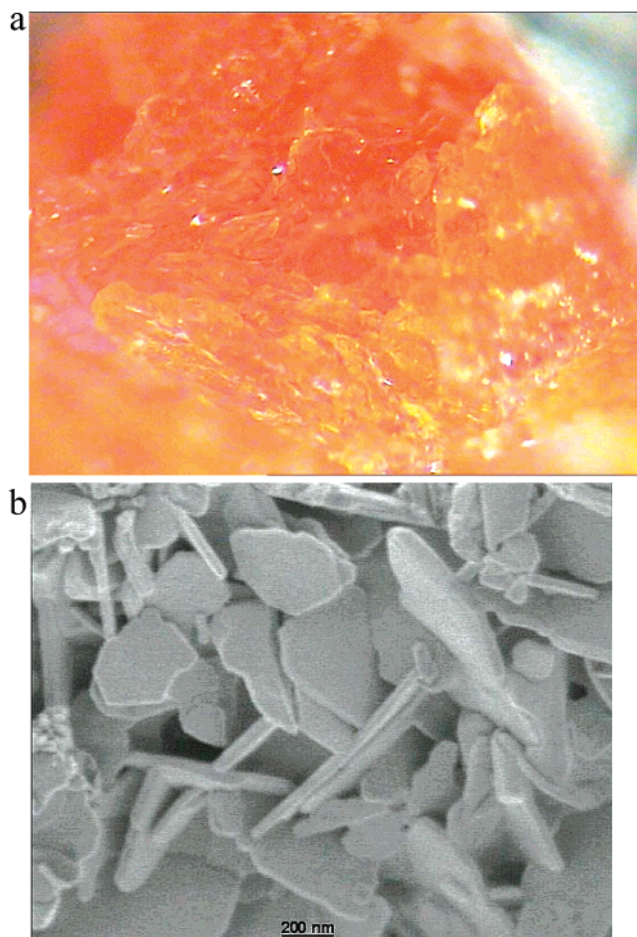areas. The decomposition of the nitrates led to platelet-shaped particles, as can be see in the scanning electron micrograph (Figure 3).

In the citrate and tartrate precursor processes, co-agulated products of perovskite nanoparticles (see Figure 4) were formed.

The lanthanum cobaltate powders with the smallest and most homogeneous distribution of particle diameter were synthesized in the reverse microemulsion process (see Figure 5). The particle size of these product is related to the droplet size of the emulsion and can therefore be varied more precisely. In the transmission electron micrographs (shown in Figure 5b), it can be seen that the particles were crystalline up to their outer boundaries.

The lattice parameters of the lanthanum cobaltate unit cell obtained from refinements of the XRD patterns for different synthesis methods and substitution rates are summarized in Table 1. The $(La, Er)_{1-x}(Ca, Sr)_x$ CoO_3 compounds had cubic or rhomboedral crystal structures, depending on the synthesis procedure and substitution at the A site. Simulations of the XRD patterns for possible rhomboedral and cubic phases of the $La_{0.6}Ca_{0.4}CoO_3$ perovskite are shown in Figure 6. The cubic phase was found more often for highly substituted lanthanum cobaltates. For some samples, a small broadening of the peaks at high 2θ values was found. This broadening originates from a slight (rhombohedral) distortion of the cubic structure, and hence, these samples are denoted as pseudo-cubic in Table 1.
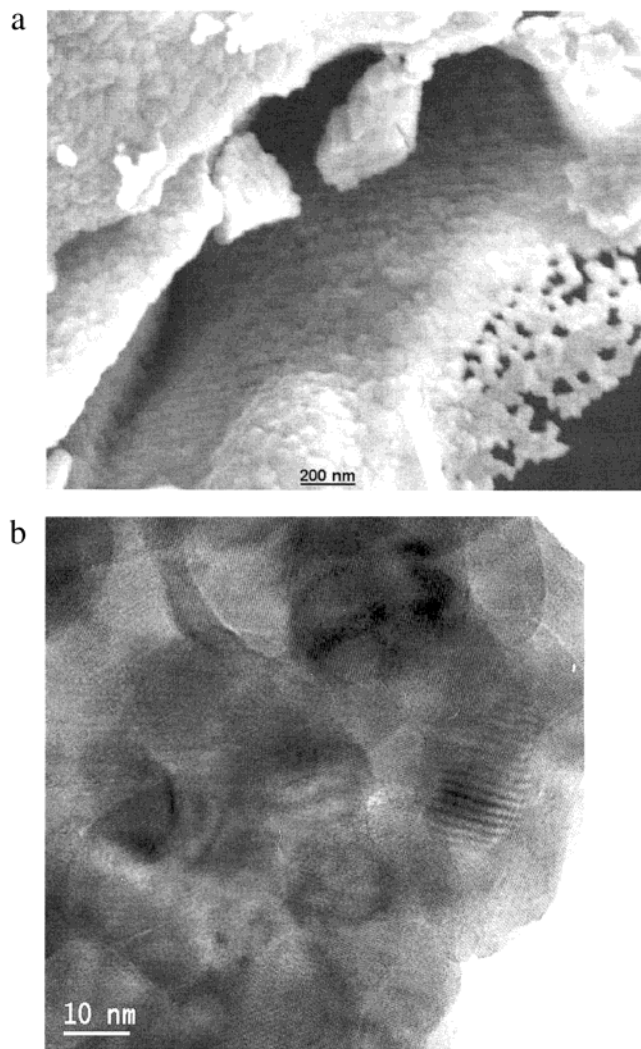
Ln₁₋ₓAₓCoO₃/Carbon Nanotube Composite Materials

Chem. Mater., Vol. 14, No. 4, 2002 **1801**

Figure 4. (a) Scanning and (b) transmission electron micrographs of $La_{0.6}Ca_{0.4}CoO_3$ prepared from a tartrate precursor.

Figure 5. (a) Scanning and (b) transmission electron micrographs of $La_{0.6}Ca_{0.4}CoO_3$ prepared by a microemulsion process.

The variation of the lattice parameters can be explained by the ion-radius mismatch with the ions substituting at the rare earth site (see also refs 4 and 10). The cell parameter *a*, for example, decreases with increasing Ca content, as the ionic radius of the Ca ion is smaller than the radii of the La, Sr, and Ba ions.[11]

The structural distortion of the ideal cubic phase of the perovskite structure is a function of the size of the substituting rare earth or alkaline earth ion (see Table 2) and the temperature (oxygen stoichiometry).

The cation substitution at the La sites leads to different ion and vacancy ordering. This can result in enormous variations in the catalytic activity. The correlation between A-site substitution by Sr or Ca and catalytic activity was shown for manganites in ref 12. It was found that the activity increases with increasing substitution.

Transmission electron micrographs (Figures 4b and 5b) of perovskite nanoparticles with the composition
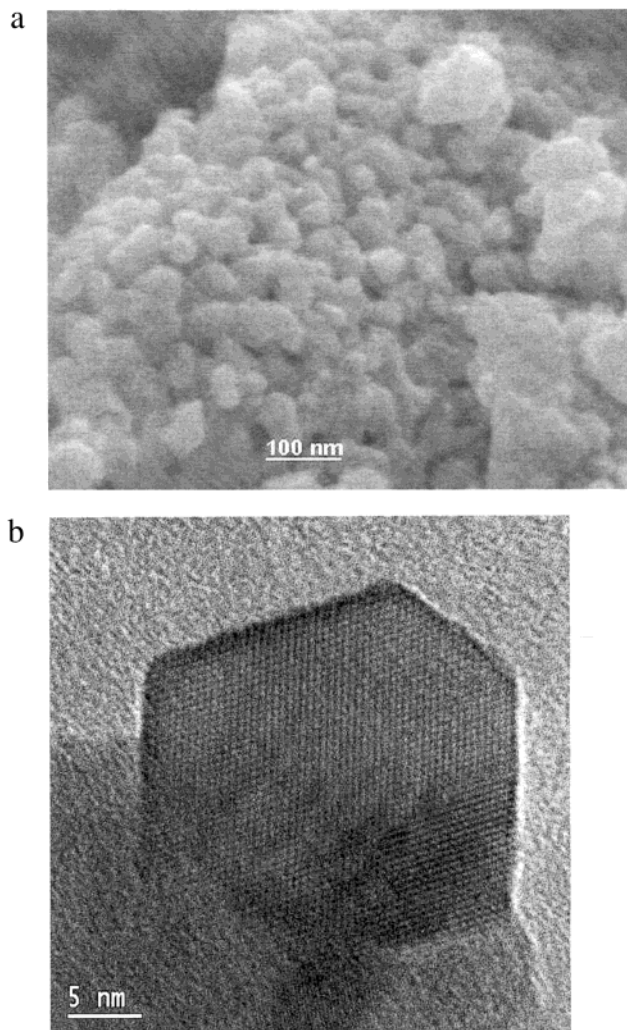
$La_{0.6}Ca_{0.4}CoO_3$ show that the particles are well-crystallized and that the particles, as well as the coherent crystalline domains, are 20 nm in diameter. The superstructures that can be found in micrographs of some substituted lanthanum cobaltate particles are probably a consequence of oxygen-deficient domains with a brownmillerite structure.[13]

Phase Stability. The structural changes in the crystal were monitored by high-temperature XRD and TA including DSC.

It was found by Ohno et al.[4] that, with increasing La substitution in the range $0 < x < 0.4$, the catalytic activity of the lanthanum cobaltates increases. Surprisingly, the activity of the compound with $x = 0.5$ was lower than that of the compound with $x = 0.4$.

In our experiments, it was not possible to prepare a $La_{0.5}Ca_{0.5}CoO_3$ monophase by ceramic synthesis. Therefore, we tested the thermal stability of the perovskite particles produced by the amorphous precursor route by monitoring the changes in the XRD pattern after heating the products to 1000 °C for several hours in air (see Figure 7).

The perovskite structures of the samples with compositions $La_{0.8}Ca_{0.2}CoO_3$ and $La_{0.6}Ca_{0.4}CoO_3$ sustained

(10) Ganguly, R.; Gopalakrishnan, I. K.; Yakhmi, J. V. *Physica B* **1999**, *271*, 116−124.

(11) Shannon, R. D.; Prewitt, C. T. *Acta Crystallogr.* **1969**, *B25*, 925−946.

(12) Isupova, L. A.; Tsybulya, S. V.; Kryukova, G. N.; Alikina, G. M.; Boldyreva, E. V.; Yakovleva, I. S.; Ivanov, V. P.; Sadykov, V. A. *Solid State Ionics* **2001**, *141−142*, 417−425.

(13) Baiker, A.; Marti, P. E.; Keusch, P.; Fritsch, E.; Reller, A. *J. Catal.* **1994**, *146*, 268−276.

Table 1. Structure and Unit Cell Dimensions of the Produced Perovskites

name	phase composition	synthesis method	XRD	parameter of (pseudo)cubic cell a_{cub} (Å)	a_{rho} (Å)	α (°)
ErZi 3	$Er_{0.6}Ca_{0.4}CoO_3$	citrate	cub	3.819		
LCC112	$La_{0.5}Ca_{0.5}CoO_3$	citrate	cub	3.816		
LCC14	$La_{0.5}Ca_{0.5}CoO_3$	citrate	cub	3.815		
LCC115	$La_{0.6}Ca_{0.4}CoO_3$	citrate	pseudo-cub	3.820		
LCC115a	$La_{0.6}Ca_{0.4}CoO_3$	coprecipitation	cub	3.817		
LCC116	$La_{0.6}Ca_{0.4}CoO_3$	citrate	cub	3.817		
LCC18	$La_{0.6}Ca_{0.4}CoO_3$	tartrate	pseudo-cub	3.822		
LCC21B	$La_{0.6}Ca_{0.4}CoO_3$	citrate, PEG	cub	3.821		
Zi 1	$La_{0.7}Ca_{0.3}CoO_3$	citrate	cub	3.822		
LCC13	$La_{0.8}Ca_{0.2}CoO_3$	citrate freeze-dried	cub	3.825		
LCC111	$La_{0.8}Ca_{0.2}CoO_3$	citrate	rho		5.376	60.66
LCC2	$La_{0.8}Ca_{0.2}CoO_3$	ceramic	rho		5.376	60.60
LC2	$LaCoO_3$	ceramic	rho		5.377	60.79
LC8	$LaCoO_3$	citrate freeze-dried	pseudo-cub	3.830		
LSC1	$La_{0.6}Sr_{0.4}CoO_3$	ceramic	pseudo-cub	3.836		
LSC3	$La_{0.6}Sr_{0.4}CoO_3$	nitrate	cub	3.838		
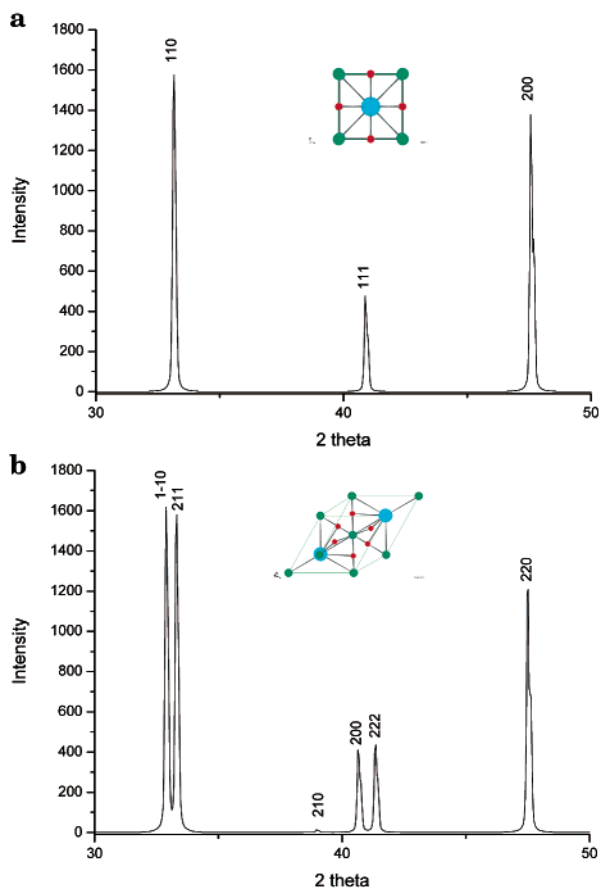
Figure 6. Simulated XRD patterns for $La_{0.6}Ca_{0.4}CoO_3$: (a) cubic, (b) rhomboedral.

the thermal treatment for more than 24 h. The particle size increased because of the sintering of small particles, as can be seen in the decreasing peak width (fwhm) of the XRD peaks.

As shown in the XRD patterns of Figure 7a, the $La_{0.8}Ca_{0.2}CoO_3$ phase had a distorted cubic structure before and a rhomboedral structure after the thermal treatment. The cubic structure $La_{0.6}Ca_{0.4}CoO_3$ remained after the thermal treatment (see Figure 7b).

Substitution of 50% of the lanthanum content by Ca led to a metastable product with the composition $La_{0.5}Ca_{0.5}CoO_3$. After this compound was heated at $T = $ 1000 °C for 10 h, a secondary Ca-rich phase appeared in the XRD (see Figure 7c).

Table 2. Experimental Results of Selected Perovskites for the Carbon Nanotube/Metal Oxide Composite Production[a]

catalyst system	synthesis procedure[b]	reaction temp (°C)	CNT growth rate (wt %/min)
LCC0 $La_{0.6}Ca_{0.4}CoO_3$	citrate	700	69.5
LCC2 $La_{0.6}Ca_{0.4}CoO_3$	tartrate	700	90.3
LCC3 $La_{0.8}Ca_{0.2}CoO_3$	ceramic	700	3.2
LCC1 $La_{0.6}Ca_{0.4}CoO_3$	impr ceram	780	16.7
LCC1 $La_{0.6}Ca_{0.4}CoO_3$	impr ceram	800	15.8
LC6 $LaCoO_3$	cotton fiber	800	40.1
LC0 $LaCoO_3$	ceramic	800	0.8
LCC10 $La_{0.5}Ca_{0.5}CoO_3$	citrate	800	43.3
LSC3 $La_{0.6}Sr_{0.4}CoO_3$	citrate	600	5,2
LC8 $LaCoO_3$	citrate	600	0.7
LCC13 $La_{0.8}Ca_{0.2}CoO_3$	citrate	800	29.7
LSC14 $La_{0.6}Sr_{0.4}CoO_3$	citrate	800	9.9

[a] Reaction time = 5 min, carbon source = 100 mL/min acetylene. [b] Perovskite precursors produced by ceramic methods, impregnation of coarse particles, the Pechini process, or the cotton-templated method.

The crystallographic structures of the compounds could be varied by altering the synthesis procedures, for example, by using different cooling rates. Because the physical properties are directly related to the structure, it is of importance that the preparation conditions be thoroughly controlled for the desired phase to be obtained and, in turn, for the reactivity to be optimized.

In the HT-XRD experiments, the phase transition from the cubic to the rhomboedral perovskite structure could be monitored in situ by observing, for example, the (110) peak splitting.

Heating cubic $La_{0.6}Ca_{0.4}CoO_3$ powder on a Pt band to 600 °C with intermediate measurements in 100 °C steps led to the formation of a rhomboedral perovskite structure at 300–400 °C (see Figure 8). Above 400 °C, a thermally expanded cubic structure was formed. During cooling, the structural changes were observed in the same temperature range as during heating, indicating the reversibility of the phase transitions cubic ↔ rhomboedral ↔ cubic.

With DSC measurements, endothermic transitions (11kJ/mol) were detected at 300 and 380 °C.

Reactivity. Substituted lanthanum cobaltates are known to be catalysts for several redox reactions. Our aim was to optimize the electrode material by increasing its reactivity. Therefore, the reactivities of the produced
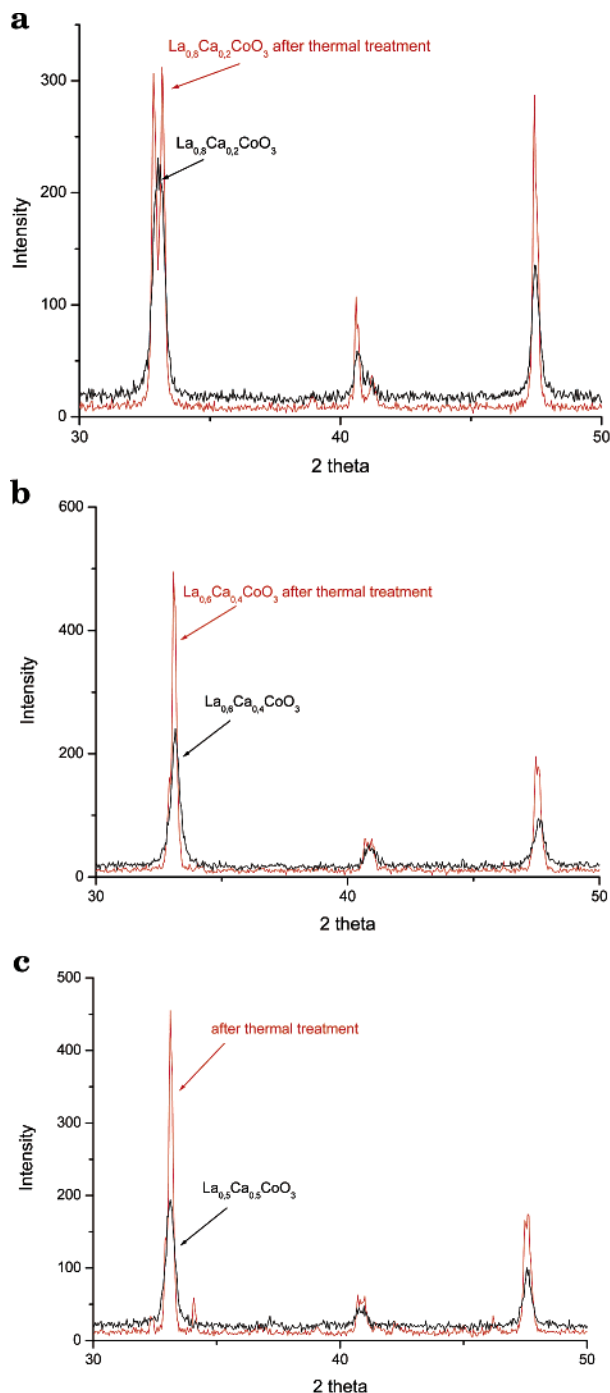
a

b

c

Figure 7. XRD patterns for the compounds (a) $La_{0.8}Ca_{0.2}CoO_3$, (b) $La_{0.6}Ca_{0.4}CoO_3$, and (c) $La_{0.5}Ca_{0.5}CoO_3$ before and after the heat treatment.

Figure 8. Part of the XRD pattern of $La_{0.6}Ca_{0.4}CoO_3$ and Si at 23, 200, and 600 °C (Ni cathode).

therein. Perovskite micro- and nanoparticles with the compositions $La_{1-x}(Ca, Sr)_xCoO_3$ and the amorphous precursors for these compounds were used as catalysts for the growth of carbon nanotubes. The nanoclusters of cobalt formed on the surface of the perovskite particles during nanotube growth were prevented from agglomeration because they were fixed in the matrix of the metal oxide. This led to suitable nucleation sites for the growth of nanotubes.

In Table 2, some of the active perovskites and their catalytic performances at different temperatures are listed. The reactivity toward hydrocarbon cracking varies for the applied cobaltates from a CNT growth rate of nearly 0 to a rate of 90 wt % per minute. The composition and texture of the catalyst determines the product quality and yield. It was found that Ca-substituted lanthanum cobaltates are more active than Sr-substituted lanthanum cobaltates and pure $LaCoO_3$. Nanoparticles from the amorphous precursor process or the precursors themselves produced more carbon nanotubes than coarse products from the ceramic synthesis.

The TEM and SEM images of the products reveal that the formed multiwalled carbon nanotubes (MWNTs), consisting mainly of nested carbon nanotubes, had a length of approximately 20 μm (see Figure 9) and diameters in the range of 20−30 nm. Some of the encapsulated particles were identified as metallic Co by EDX point analysis. EXAFS measurements of isolated carbon nanotubes confirm this result.[15] The data clearly show that, during the reaction, the perovskite structure was partially destroyed.

In additional experiments, coarse perovskite materials with particles of several microns in diameter, formed in ceramic or coprecipitation processes, were used. The particles were initially impregnated with a precursor solution containing the appropriate stoichiometric citrate mixture with an excess of 5% cobalt. The excess Co formed the nucleation sites for carbon nanotube growth, and the higher bulk-to-surface ratio prevented the bulk perovskite phase from decomposing. With these precursors it was possible to grow carbon nanotubes on the surface only of the particles in a very short reaction time (3 min). The transmission and scanning electron micrographs of the product are shown in Figure 10.

Macrostructured lanthanum cobaltates from the combustion synthesis with cotton fibers were used for the

compounds were tested in two different processes: (1) The catalytic properties were tested in a hydrocarbon cracking reaction to form carbon nanotubes and hydrogen. (2) The electrocatalytic properties were tested in an oxygen electrode for their application in zinc/air batteries.

Cracking of Hydrocarbons. Cobalt incorporated in metal oxides can serve as a catalyst for the formation of carbon nanotubes (CNTs), as was shown for different metal oxides in refs 9 and 14 and references cited
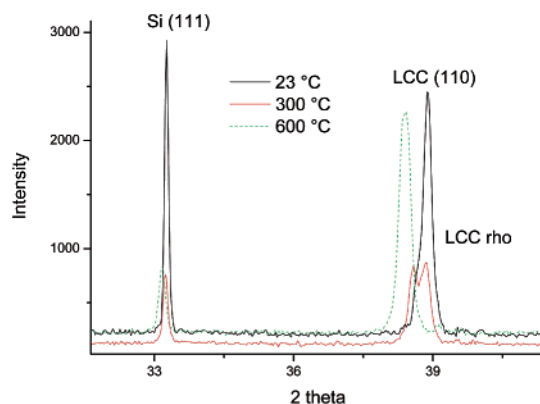
(14) Meier, A.; Kirilov, V.; Kuvshinov, G. G.; Steinfeld, A.; Weiden-kaff, A.; Reller, A.; Mogilnykh, Y. I. *Chem. Eng. Sci.* **1999**, *54*, 3341−3348.

(15) Weidenkaff, A.; Ebbinghaus, S. G. EXAFS measurements on LCC−CNT composite material. Unpublished work, 2001.
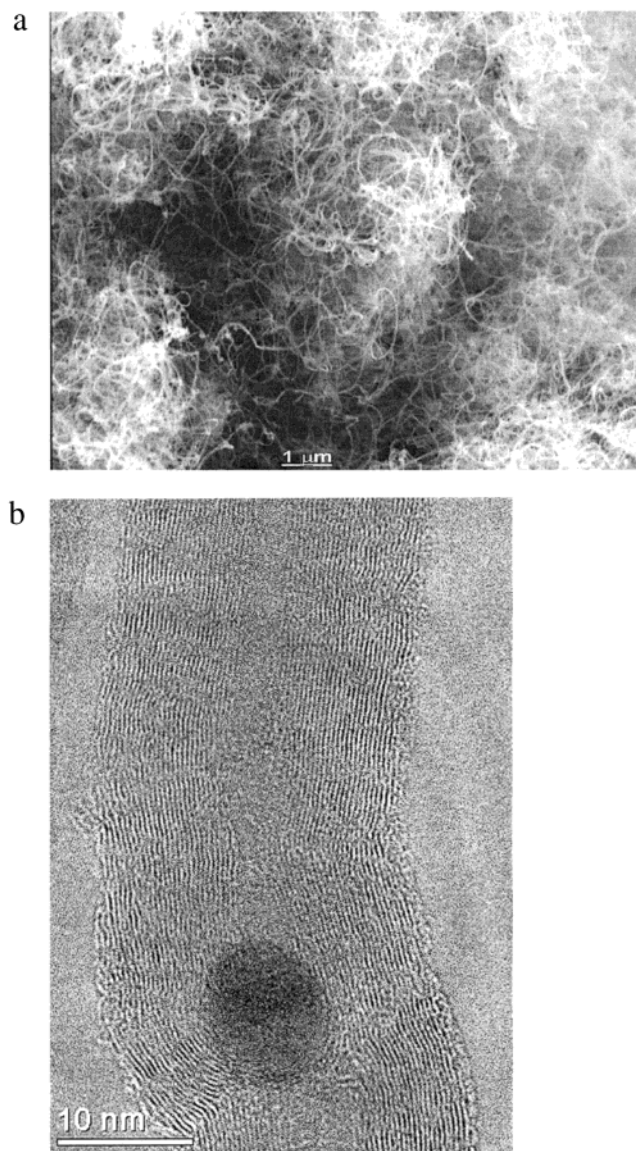
a

b

Figure 9. (a) SEM and (b) HRTEM images of multiwalled carbon nanotubes/perovskite nanocomposite material (CMC). Carbon nanotubes are enclosing the metal oxide particles.

a

b

Figure 10. (a) SEM and (b) HRTEM images of multiwalled carbon nanotube/perovskite nanocomposite (CMC). Carbon nanotubes were grown on the surface of the perovskite particles.

Figure 11. SEM image of cotton-fiber-templated carbon nanotube/perovskite nanocomposite (CMC).

production of a macrostructured nanocomposite material. The shape of the cotton fiber remained, and carbon nanotubes were grown on the surface of the lanthanum cobaltate (see Figure 11).

Electrocatalytic Reactivity. The carbon nanotube/ metal oxide nanocomposite (CMC) was used to produce an air electrode that could be used, for example, for a rechargeable zinc/air battery. The material consisted of 50 wt % multiwalled carbon nanotubes (30−40 nm in diameter) enclosing 50 wt % metal and metal oxide nanoparticles (10−20 nm in diameter). The new CMC electrode was used to compare the performance of the new nanocomposite material with that of a common composite electrode material. The comparative electrode (developed at PSI) consisted of graphite particles mixed with perovskite nanoparticles from the same production batch as used for the synthesis of the composite material (LCC170). A first test (see Figure 12) showed comparable performance between the two materials. It can be seen that the state-of-the-art electrode developed at PSI (mixed LCC170/carbon black material) was only slightly
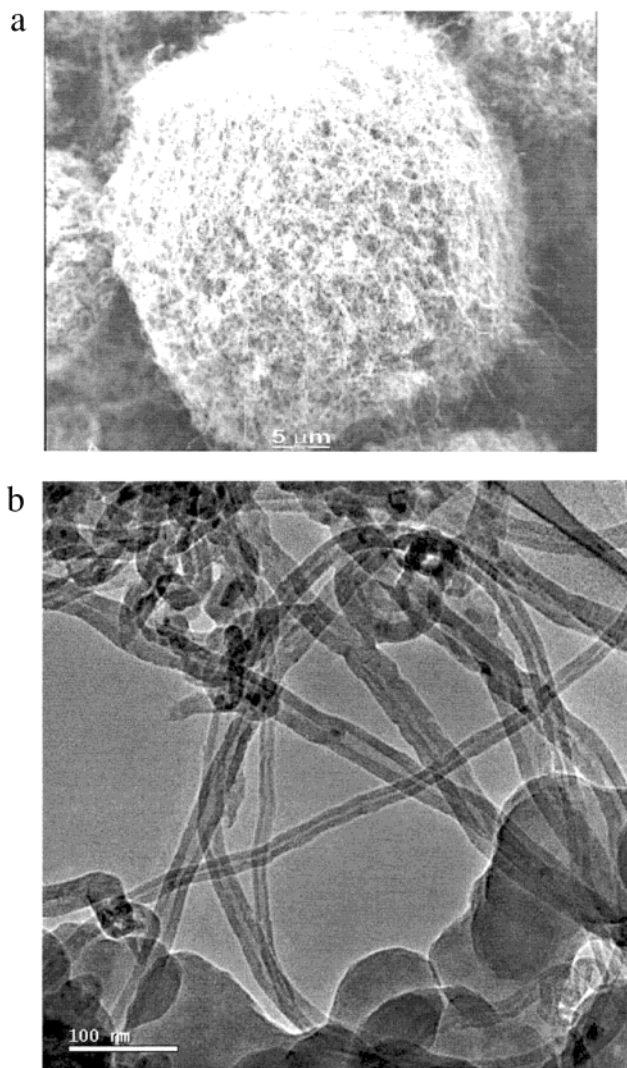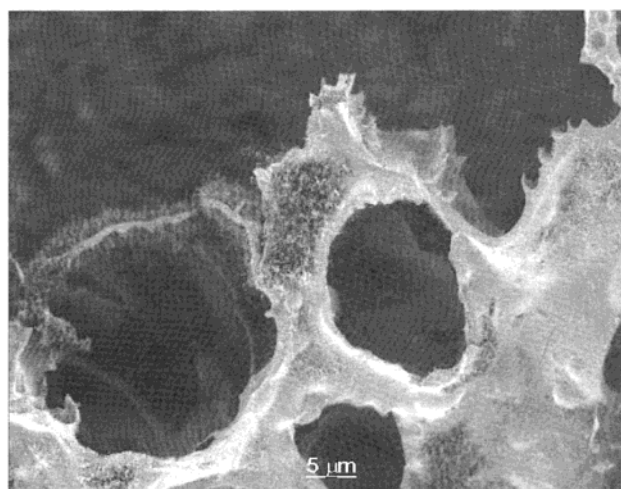
better. This result is very promising: Although the catalytically active oxide was partly destroyed (i.e., reduced to metallic Co) during the growth of the carbon nanotubes, the electrode showed almost the same activ-
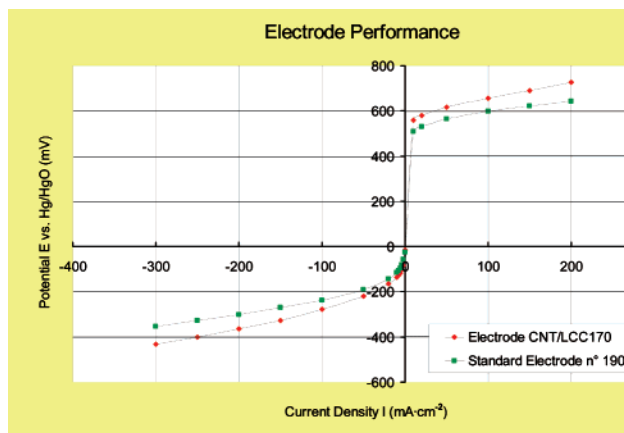
Figure 12. Current density vs potential plot for the standard PSI and CNT/LCC electrode in 1 M KOH.

ity as the best electrode produced thus far by mixing the perovskite with graphite. To improve the performance of the new CMC electrode, a material with intact perovskite structure has to be developed. We believe that a modification of the preparation techniques leading to intact perovskite material covered with carbon nanotubes (see considerations above) will further increase the reactivity of the electrodes. Consequently, these new composite materials are highly interesting candidates for technical applications in oxygen electrodes.

The electrocatalytic reactivity of the perovskites was tested in a four-probe arrangement with single-crystalline thin films of $La_{1-x}Ca_xCoO_{3-\delta}$ grown on an inert substrate material to avoid the influence of grain boundaries and the substrate material. The results of these comparative measurements are described elsewhere.[16]

Conclusions

Micro- and nanoparticles with the composition (La, Er)$_{1-x}$(Ca, Sr, Ba)$_x$CoO₃ ($x = 0$, 0.2, 0.4, and 0.5) were successfully prepared by ceramic, coprecipitation, and complexation methods. The compounds have either a cubic or rhomboedral perovskite structure and very different morphologies.

(16) Montenegro, M. J.; Lippert, T.; Müller, S.; Weidenkaff, A.; Willmott, P. R.; Wokaun, A. Deposition of electrochemically active perovskite films. *Appl. Surf. Sci.*, in press.

Coprecipitation in microemulsions was found to be the best technique for producing nanoparticles with the desired homogeneous particle size distribution. The disadvantage of this process is the very small yield of perovskites and the large amount of organic waste material.

The XRD patterns of the substituted cobaltates at different temperatures in HT-XRD experiments showed a reversible structural transition in air.

The results of the electrochemical measurements on the new electrode material were promising, even though the overpotential of the electrode was not decreased.

The electrical properties of carbon nanotubes are different from those of graphite nanoparticles, and it was shown in TGA experiments and wet chemical experiments (see also ref 9) that the thermal and chemical stability of carbon nanotubes is higher than that of graphite nanoparticles, so that a better cycling performance for this material can be expected in further tests with improved CMC materials. Carbon nanotubes grown directly on the perovskite material can improve the electrical junction between the oxide and the carbon-containing substrate.

For enhanced catalytic performance (electrical and chemical), small particles with a large surface area are advantageous, but the drawback for improved reactivity is a lower stability of the compounds. If the particles are too small, the structure can be destroyed during a thermal or chemical treatment, such as the growth of the carbon nanotubes. With the developed synthesis methods, the particle size and surface texture of the metal oxide particles can be designed to provide both a maximum surface area and a stable structure. This development can be applied to enhance the efficiency of Zn/air batteries.